Available online at www.sciencedirect.com

SciVerse ScienceDirect

Procedia Engineering 39 (2012) 98 – 110

Procedia Engineering

www.elsevier.com/locate/procedia

XIIIth International Scientific and Engineering Conference "HERVICON-2011"

Ideal Material Models for Engineering Calculations

Jerzy Bochnia[a] a*

[a]*Kielce University of Technology, Mechanical Technology and Metrology, Al. 1000-lecia P.P. 7, 25-314 Kielce, Poland*

Abstract

The two main objectives of this study were: 1) to analyze the effect of the coefficient of damping of the seal material on its operation parameters (simulation) and 2) to describe the selected engineering material (polyurethane) by means of the Standard II material model.

Keywords: Face contacting seal; rotor; coefficient of damping; rheological models.

1. Introduction

The safety of machine components is largely dependent on the mechanical properties of materials, e.g. tensile strength, yield strength, fatigue strength, impact strength and hardness, which are treated as static and dynamic indicators. With the knowledge of what affects the mechanical properties, engineers are able to solve various problems, which usually implies selecting an appropriate material to be used under specified mechanical load conditions.

Mechanical, and particularly rheological properties, can be characterized using ideal material equations. An ideal material is represented by a mechanical model of a given continuum. The mechanical model is the representation of the characteristic features of this continuum by means of mechanical components, e.g. a spring, a hydraulic damper and a slide. The elements can be connected in series or parallel, creating multi-parameter models with different degrees of complexity. An ideal material is described with a constitutive equation that is usually a relation between the force acting upon the ideal material and the effect of this force, i.e. the resulting displacement. The relationships between stress and strain are also considered.

* Corresponding author. *Tel:* +48 41 3424756.
E-mail address: jbochnia@tu.kielce.pl.

1877-7058 © 2012 Published by Elsevier Ltd. Open access under CC BY-NC-ND license.
doi:10.1016/j.proeng.2012.07.013

Developing equations of complex rheological models is very troublesome; it is thus common to use a method that involves introducing universal symbolic notation for the relations between the force and the strain [1]. As the relationships are differential, the differential operators Π and Γ need to be introduced. They provide us with an appropriate formula for performing the operation of differentiation of force and strain in the function of time. The relation between force P and strain x in the notation with a differential operator is as follows:

$$\Pi P(t) = \Gamma x(t)\,. \tag{1}$$

In algebraic transformations, the differential operators are treated as algebraic quantities, which implies that they can be used in algebraic operations. For models connected in parallel, we use a procedure similar to that used for a parallel connection of springs. The equations of ideal materials applied in engineering calculations replace the equation of a real material. As a result, it is possible to simulate the operation of various engineering systems.

Ideal material models can be applied in practice if their constitutive equations can be used to describe a real solid material. Polymers, especially polyurethane polymers, are an example of engineering materials that can be described in this way [2,3]. Polyurethanes are engineering materials representing continua that combine the properties of solids and liquids. To develop the characteristic of the real material using the equations of the ideal material models, it is necessary to conduct a load test on the samples of the real material. The test results in the form of curves showing changes in the load force in the function of time are then used to identify the coefficients of the ideal material equation in order to describe the real material.

The two main objectives of this study were: 1) to analyze the effect of the coefficient of damping of the seal material on its operation parameters (simulation) and 2) to describe the selected engineering material (polyurethane) by means of the *Standard II* material model.

2. Influence of the mechanical properties of the seal material on the parameters of its operation

2.1. Model of the dynamics of the sealing ring

Many recent papers dealing with the dynamics of face seals, e.g. Refs. [4, 5, 6], treat sealing rings as ideal rigid bodies.

This paper is concerned with the dynamics of a face sealing ring resulting from the predetermined disturbances of the primary motion of a turbomachine and the influence of the mechanical properties of the ring on the parameters of its operation. This study is a continuation and slight extension of Refs. [7,8]. In dynamic mechanical analysis, the mechanical properties of structural elements, for instance, the nonlinear influence of the elasticity of the ring material on the ring vibrations, are frequently taken into account [9].

A sealing ring is commonly made of plastic with nonlinear viscoelastic properties, e.g. polyurethane, rubber or polymer composites. A schematic diagram of the analyzed sealing ring is shown in Fig. 1. The sealing ring separates space A from space B. Figure 1a illustrates the position of the seal elements at no-disturbance condition, while Fig 1b illustrates their position affected by angular disturbances.

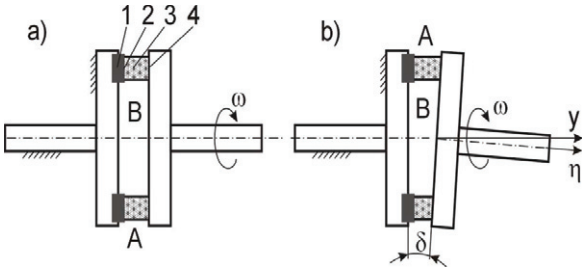

Fig. 1. A face contacting seal. 1 – stator, 2 – sliding surfaces, 3 – rotor, 4 – fastening surface

A sealing ring is pressed against a sliding surface with a constant force. Disturbances to the primary motion of the system cause that the axis of the seal rotor deviates by a certain, usually time-variant, angle $\delta(t)$, which leads to deformations of the sealing ring and its non-uniform pressure against the sliding surface. The pressure of the ring against the sliding surface prevents leakage of the medium between space B and space A. The sealing ring should be pressed against the sliding surface with a force larger than that required at the no disturbance condition. As a result the temperature rises due to friction and the wear of the ring is greater. In special cases, the vibrations of the ring material can be so strong that the seal will fail.

It is significant to analyze the vibrations of the sealing ring considered as a continuum with combined mechanical properties. The problem solution depends on the formulation of the calculation model with effective simplifications. The sealing ring is initially pressed against the sliding surface with a constant force, P, causing initial stresses and strains, called initial condition. While the system moves, some small vibrations occur around that condition. They can be described linearly.

The main assumption of the model was that the material used for the sealing ring was characterized by generalized linear mechanical properties for small vibrations around the initial operating condition. As a result, the axial strains of the ring become independent of the torsional strains. It was assumed that the rheological properties of the material used for the ring would be described by the *Standard II* ideal material model, presented in Fig. 2.

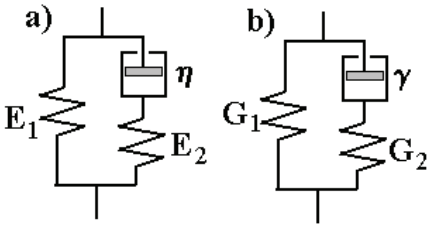

Fig. 2. *Standard II* – the ideal material model used for describing the material for a sealing ring

The model was simplified by decomposing the strains. The sealing ring was separated into elementary rings (Figs. 3a and b), and then further into elementary segments (Figs. 3c and d). It was assumed that during deformations the segments did not affect each other. This assumption involves some risk. It is essential not to consider the spatial stress condition; instead, it is reduced to the superposition of one-dimensional conditions, which considerably simplifies further analysis. Errors resulting from these simplifications are not easy to assess. Further studies will focus on determining these errors through experiments. The axial strains of the ring were thus reduced to the longitudinal strains of the segments,

while the ring torsion to transverse strains, determined like bending due to non-dilatational strains only. By solving such a model, it is possible to determine the pressure of the ring against the sliding surface and to determine the friction forces and the non-dilatational strain of the ring, i.e. its torsion by using a suitable hypothesis of friction.

Another objective was to formulate the direction of the vector of the driving torque applied to the shaft where the sealing ring is used. Two variants are possible here (Fig.1): a) a vector of that torque coincides with the y-axis – the torque does not follow the deviations of the shaft axis and b) a vector of this torque coincides with the moving η-axis - the torque follows the deviations of the shaft axis. The latter case is much more difficult to solve. Further considerations will be based on variant a).

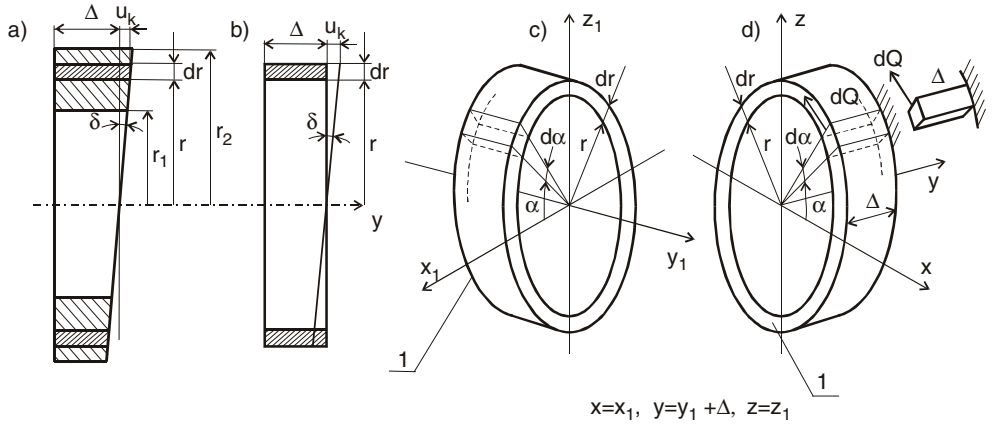

Fig. 3. Model of the sealing ring [8]

2.2. Axial and transverse vibrations of the sealing ring

Only the final solution is presented here. The derivation of the equation is described in Ref. [8]. The considerations focused on the longitudinal vibrations of the elementary segment with length Δ and the area of the cross-section r dr dα, which was separated from the sealing ring. The vibrations were due to the kinematic excitation, which was attributable to the rotary motion and the deviation of the rotor axis (Fig. 1b). The equation of the longitudinal vibrations of the elementary segment, presented in Fig. 4, for small strains is as follows [8]:

$$\frac{\eta}{E_2}\frac{\partial^3 u}{\partial t^3}+\frac{\partial^2 u}{\partial t^2}-\frac{\eta}{\rho}(1+\frac{E_1}{E_2})\frac{\partial^3 u}{\partial y^2 \partial t}-\frac{E_1}{\rho}\frac{\partial^2 u}{\partial y^2}=-\frac{y}{\Delta}r[q(t)+\frac{\eta}{E_2}\frac{dq(t)}{dt}], \tag{2}$$

where:

$$q(t)=[\ddot{\delta}(t)-\omega^2\delta(t)]\sin(\omega t+\alpha)+2\omega\dot{\delta}(t)\cos(\omega t+\alpha). \tag{3}$$

The equation was solved using the one-dimensional Bubnov-Galerkin method [10]. With regard to variable y, it was assumed that:

$$u(y,t)\approx Y(y)S(t) \tag{4}$$

and

$$Y(y) = \sin \kappa y\,, \tag{5}$$

where: $\kappa = \frac{\pi}{\Delta}$. According to this method, we obtain:

$$\frac{\eta}{E_2}\dddot{S}(t) + \ddot{S}(t) + \kappa^2 \frac{\eta}{\rho}(1 + \frac{E_1}{E_2})\dot{S}(t) + \kappa^2 \frac{E_1}{\rho} S(t) = e(t)\,, \tag{6}$$

where:

$$e(t) = \frac{2r\omega^2\delta}{\pi}[\sin(\omega t + \alpha) + \frac{\eta}{E_2}\omega\cos(\omega t + \alpha)]\,. \tag{7}$$

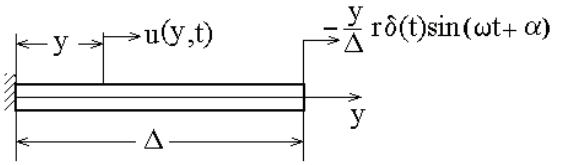

Fig. 4. An elementary segment separated from the ring [8]

Equation (6) can be solved by using a digital method for variable δ(t). An analytical solution is possible when $\delta(t) \approx \delta = const$ and $\kappa = \pi / \Delta$. Harmonic excitation and damping cause that at $\delta = const$, the process of vibrations stabilizes. During the steady-state process, the system will vibrate harmonically with frequency ω. That is why a solution in the following form was sought:

$$S(t) = rA\cos\omega t + rB\sin\omega t\,, \tag{8}$$

where: A and B are constants determined from the system of algebraic equations.

The stress resulting from the ring vibrations was [8]:

$$\sigma(0,t) = \sigma(t, r, \delta, \alpha, \omega) = rC(\delta, \alpha, \omega)\cos\omega t + rD(\delta, \alpha, \omega)\sin\omega t\,, \tag{9}$$

where: C and D are constants. (The formulas are provided below, in the calculations of the MATHCAD program).

Like in the case of axial vibrations, only ready solution is included. The derivation is presented in Ref. [8]. The transverse vibrations of the sealing ring were due to the variability in the friction forces on the sliding surface. The forces were dependent on numerous factors, including stresses σ shown above.

The equation of the transverse vibrations was derived for the elementary segments. The shape of an elementary segment is shown in Fig. 5. It was assumed that it bends only due to non-dilatational strains (tangential stresses). The ideal material model used for this analysis was *Standard II*.

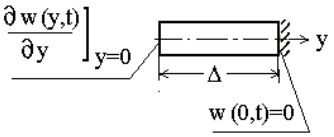

Fig. 5. Elementary segment [8]

The equation of the transverse vibrations of the elementary segments is as follows [8]:

$$\frac{\gamma}{G_2}\frac{\partial^3 w}{\partial t^3}+\frac{\partial^2 w}{\partial t^2}-\frac{\gamma}{k\rho}(1+\frac{G_1}{G_2})\frac{\partial^3 w}{\partial y^2\partial t}-\frac{G_1}{k\rho}\frac{\partial^2 w}{\partial y^2}=\frac{\mu}{\rho}[\sigma(0,t)+\frac{\gamma}{G_2}\dot{\sigma}(0,t)]\delta(y)\cdot \tag{10}$$

Like in the case of axial vibrations, the Bubnov-Galerkin method was used [10], thus:

$$\frac{\gamma}{G_2}\dddot{T}(t)+\ddot{T}(t)+\lambda^2\frac{\gamma}{k\rho}(1+\frac{G_1}{G_2})\dot{T}(t)+\lambda^2\frac{G_1}{k\rho}T(t)=\frac{2\mu}{\rho\Delta}[\sigma(0,t)+\frac{\gamma}{G_2}\dot{\sigma}(0,t)]\cdot \tag{11}$$

In the simplest friction model, the dynamic component was:

$$\tau_d=\mu\sigma(0,t)=\mu r(C\cos\omega t+D\sin\omega t)\,. \tag{12}$$

The total stress was:

$$\tau=\frac{4P\mu}{\pi(r_2^2-r_1^2)}+\tau_d\,. \tag{13}$$

2.3. Effect of the damping coefficient on the tangential stresses

By calculating the tangential stresses, one can easily determine the friction force and then the friction torque, with the latter being one of the parameters of operation of a face sliding seal.

The calculations of the tangential stresses were performed for the following data:

$E_1=3\cdot10^{10}\,N/m^2$, $E_2=8\cdot10^{10}\,N/m^2$, $G_1=1\cdot10^{10}\,N/m^2$, $G_2=2.8\cdot10^{10}\,N/m^2$, $\gamma=5\cdot10^5\,Ns/m^2$, $\rho=2000\ kg/m^3$, $\Delta=0.01\ m$, $\delta=0{,}1^o$, $\mu=0.2$, $k=1.2$, $r_1=0.02\ m$, $r_2=0.04\ m$, $\omega=600\ rad/s$, $r=0.03\ m$ i $\alpha=180^o$, $P = 10\ N$.

The following values of the damping coefficient were assumed: $\eta = 5\cdot10^2$; $5\cdot10^6$; $8\cdot10^6$; 10^7; $5\cdot10^7$; 0; $5\cdot10^{20}$; $3.65\cdot10^7\ Ns/m^2$. Some of the recorded Mathcad calculations are included below.

$$A := \frac{\left[\left(\frac{2\cdot\delta\cdot\omega^2}{\pi}\right)\cdot\left[\frac{\eta}{E_2}\cdot\omega^3 - \frac{\pi^2\cdot\eta\cdot\omega}{\Delta^2\cdot\rho}\cdot\left(1+\frac{E_1}{E_2}\right) + \frac{\pi^2\cdot E_1}{\Delta^2\cdot\rho} - \omega^2\right]\right]\cdot\left(\cos(\alpha) - \frac{\eta\cdot\omega}{E_2}\cdot\sin(\alpha)\right)}{\left[\frac{\eta}{E_2}\cdot\omega^3 - \frac{\pi^2\cdot\eta\cdot\omega}{\Delta^2\cdot\rho}\cdot\left(1+\frac{E_1}{E_2}\right)\right]^2 + \left(\frac{\pi^2\cdot E_1}{\Delta^2\cdot\rho} - \omega^2\right)^2}$$

$$B := \frac{\left[\left(\frac{2\cdot\delta\cdot\omega^2}{\pi}\right)\cdot\left[\frac{\eta}{E_2}\cdot\omega^3 - \frac{\pi^2\cdot\eta\cdot\omega}{\Delta^2\cdot\rho}\cdot\left(1+\frac{E_1}{E_2}\right) + \frac{\pi^2\cdot E_1}{\Delta^2\cdot\rho} - \omega^2\right]\right]\cdot\left(\sin(\alpha) - \frac{\eta\cdot\omega}{E_2}\cdot\cos(\alpha)\right)}{\left[\frac{\eta}{E_2}\cdot\omega^3 - \frac{\pi^2\cdot\eta\cdot\omega}{\Delta^2\cdot\rho}\cdot\left(1+\frac{E_1}{E_2}\right)\right]^2 + \left(\frac{\pi^2\cdot E_1}{\Delta^2\cdot\rho} - \omega^2\right)^2}$$

$$C := \frac{\frac{\pi}{\Delta}\cdot\left[\left[E_1 + \frac{\eta^2\cdot\omega^2}{E_2}\cdot\left(1+\frac{E_1}{E_2}\right)\right]\cdot A + \eta\cdot\omega\cdot B\right]}{1+\left(\frac{\eta\cdot\omega}{E_2}\right)^2}$$

$$D := \frac{\frac{\pi}{\Delta}\cdot\left[\left[E_1 + \frac{\eta^2\cdot\omega^2}{E_2}\cdot\left(1+\frac{E_1}{E_2}\right)\right]\cdot B - \eta\cdot\omega\cdot A\right]}{1+\left(\frac{\eta\cdot\omega}{E_2}\right)^2}$$

$$\tau_d(t) := \mu\cdot r\cdot\left(C\cdot\cos(\omega\cdot t) + D\cdot\sin(\omega\cdot t)\right)$$

where: A, B, C, D are coefficients in Eqs. (8) and (12). Figure 6 shows time-dependent changes in the tangential stress for different values of the damping coefficients.

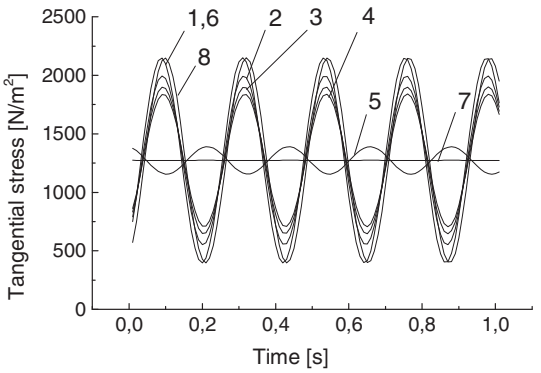

Fig. 6. Tangential stresses for different values of the damping coefficients: 1 - $\eta = 5\cdot10^2$ Ns/m^2; 2 - $\eta = 5\cdot10^6$ Ns/m^2; 3 - $\eta = 8\cdot10^6$ Ns/m^2; 4 - $\eta = 10^7$ Ns/m^2; 5 - $\eta = 5\cdot10^7$ Ns/m^2; 6 - $\eta = 0$; 7 - $\eta = 3.65\cdot10^7$ Ns/m^2; 8 - $\eta = 5\cdot10^{20}$ Ns/m^2

It was also essential to calculate the maximum tangential stresses (amplitudes) for different values of the damping coefficients. The results are shown in Fig. 7.

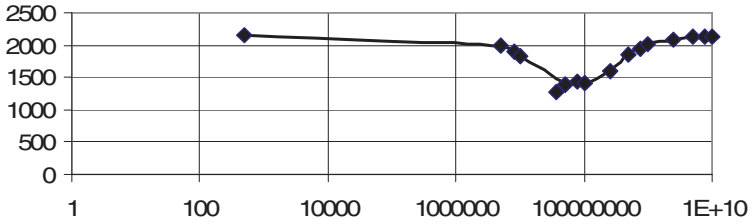

Fig. 7. Relations between the maximum tangential stresses and the values of η in the range from zero to 10^{10} Ns/m^2 (logarithmic scale). When the curve reaches a minimum, the value of the dynamic component of the tangential stress τ_d is in practice close to zero

In the analyzed model of the face seal dynamics, the rheological properties of the sliding ring are taken into account. They can be used in simulations aiming at determining the relations between the vibrations and the coefficients characterizing these properties (the damping coefficients) as well as the different effects of the pressure force and the coefficient of friction. The main advantage of applying this type of model to analyze the dynamics of a seal is that it is possible to avoid costly and labour-intensive experimental studies.

The calculation results indicate that for low as well as high values of the damping coefficient, the tangential stress reaches a maximum. Curves (6) and (8) (Fig. 6) actually coincide.

For given operation conditions of the sliding rings, there exists a certain value of the damping coefficient that causes a decrease in the amplitude of values of the tangential stresses almost to zero, as shown in the diagram in Fig. 7.

3. Determining the characteristics of selected real materials using the equation of the *standard II* ideal material model

3.1. Determining the stress relaxation of polyurethanes

Ideal material models can be applied in practice if their equations are suitable to describe a real solid material. Polymers, especially polyurethanes, are a good example of engineering materials that can be described in this way. The analysis was performed for polyurethanes (EPUR) representing continua that combine the properties of solids and liquids.

A relaxation test was conducted to determine the characteristic of the real material using the ideal material model equations. The results in the form of a curve showing the time-dependent changes in the load force were compared with the theoretical curve obtained by solving the equation describing the assumed ideal material model. The comparison results were used to calculate the coefficients characterizing this model.

The tests were performed on samples made of polyurethanes (EPUR) with the Shore hardness number of 90 and 95, using an Instron 5582 universal testing machine and equipment for static compression tests. The tests involved applying a plate that exerted a continuous load to maintain a constant depth of indentation H = 1 mm.

The stress relaxation was determined by pressing the plate against a polyurethane sample and, simultaneously, maintaining a constant depth of indentation H = 1 mm. The condition was achieved by applying the *hold extension* function of the universal testing machine involving automatic regulation of

the predetermined value of the displacement of the crossbar with the integrated plate. After indentation at a constant load rate to a predetermined depth, the plate reaches equilibrium between the external force and the internal forces – stresses. Applying the load longer would result in very slow indentation of the plate, which is related to the relaxation properties of the material. The control system of the universal testing machine controls the loading of the plate by maintaining the predetermined depth of indentation. The data acquisition system registers these changes in the function of time. To assess the stress relaxation properties of the selected engineering materials, it was necessary to maintain constant indentation H = 1 mm for a specific period of time (10 min, in this case). There was a decrease in the load F, designated as ΔF_{relaks}. The test results in the form of relaxation curves are shown in Fig. 8.

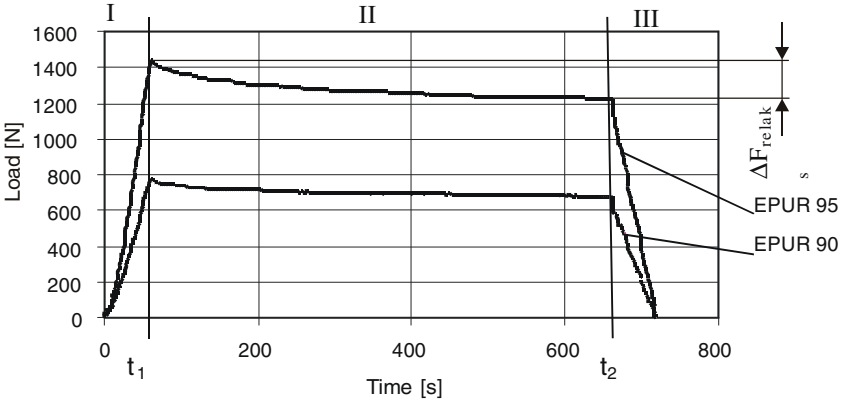

Fig. 8. Stress relaxation curves

The stress relaxation curves (Fig. 8) were divided into three areas:

I. Static loading (compression) of the polyurethane sample in time $0 \div t_1$.
II. Application of the *Hold extension* function, i.e. maintaining a constant value of strain H = 1 mm in time $t_1 \div t_2$.
III. Releasing the sample from the compressive force until zero was reached, in time longer than t_2.

Then, the next parts of the curves were analyzed, i.e. relaxation in time $t_1 \div t_2$.

3.2. Calculating the coefficients of the ideal material equation

The theoretical description was based on the *Standard II* ideal material model shown in Fig. 9.

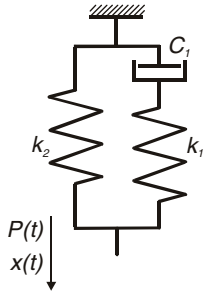

Fig. 9. *Standard II* model used for describing the analyzed polyurethanes

If the differential operators in Eq. (1) are replaced with expressions suitable for the *Standard II* model, we obtain:

$$\left(1+\frac{C_1}{k_1}\frac{d}{dt}\right)P(t)=\left(k_2+C_1\left(1+\frac{k_2}{k_1}\right)\frac{d}{dt}\right)x(t)\cdot \tag{14}$$

After transformations, the equation describing the model given in Fig. 9 is as follows:

$$\frac{d}{dt}x(t)+\frac{k_1k_2}{C_1k_1+C_1k_2}x(t)=\frac{1}{k_1+k_2}\left(\frac{d}{dt}P(t)\right)+\frac{k_1}{C_1k_1+C_1k_2}P(t) \quad . \tag{15}$$

In the relaxation process, we have: x(t) = const, thus we obtain:

$$\frac{k_1}{C_1}\frac{1}{k_1+k_2}P(t)+\frac{1}{k_1+k_2}\left(\frac{d}{dt}P(t)\right)=\frac{k_1}{C_1}\frac{1}{k_1+k_2}k_2x\cdot \tag{16}$$

After integration we get:

$$P=\frac{-\left[\exp\left(-ta_r+\ln\left(-a_rxk_1\right)\right)-a_rk_2x\right]}{a_r}, \tag{17}$$

where: $a_r=\frac{k_1}{C_1}$.

The coefficients of the above equation were determined using the given-find block of the Mathcad program for the following experimental data obtained during the relaxation test for EPUR 95:

x = 0.001 m;
P1 = 1434.65 N, t = 62 s;
P3 = 1263.62 N, t = 400 s;
P4 = 1233.21 N, t = 662 s.

The calculated values of the coefficients were: $k_1 = 1.85\cdot10^5$ N/m, $k_2 = 1.206\cdot10^6$ N/m and $C_1 = 6.331\cdot10^7$ Ns/m. After substitution into Eq. (17), they adjusted the general solution to the specific real material, describing it with the required accuracy. The solution results were presented in the form of a graph in Fig. 10.

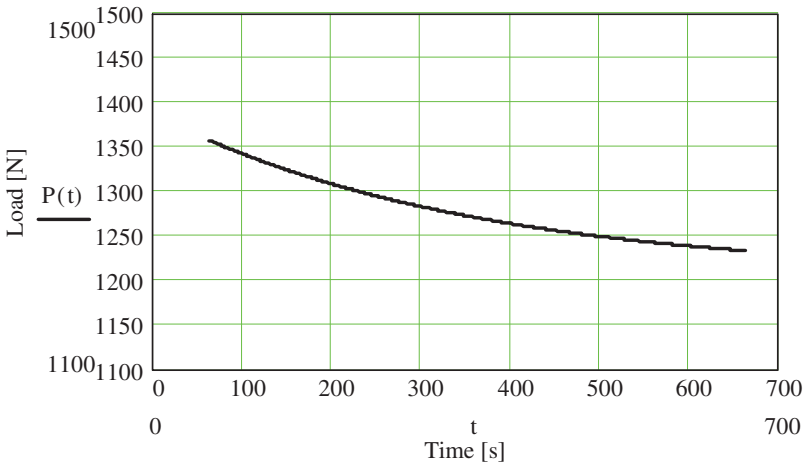

Fig. 10. Theoretical stress relaxation curve of the *Standard II* ideal material model describing the EPUR 95 material.

The theoretical and experimental relaxation curves are compared in Fig. 11.

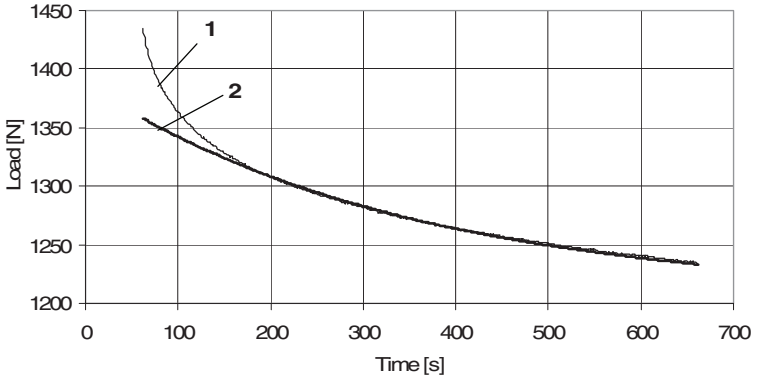

Fig. 11. Stress relaxation curves: the theoretical curve for the *Standard II* ideal material model and the experimental curve, both describing EPUR 95

As shown in Fig. 11, the *Standard II* model with the predetermined coefficients, i.e. $k_1 = 1.85 \cdot 10^5$ N/m, $k_2 = 1.206 \cdot 10^6$ N/m and $C_1 = 6.331 \cdot 10^7$ Ns/m describes EPUR 95 quite well. For most of the range, the curves coincide, however, some differences occur in the first seconds of the process. At the beginning of the process, the difference was approximately 5.4 % and it gradually diminished to a few hundredths of a percent.

The same procedure was used for EPUR 90. The coefficients of the equation of relaxation were determined using the given-find block. The following experimental data obtained from the relaxation test for EPUR 90 were analyzed:

x = 0.001 m;
P1 = 747.09 N, t = 100 s;
P2 = 720.85 N, t = 200 s;
P4 = 690.03 N, t = 600 s.

The comparison of the theoretical and experimental stress relaxation curves is presented in Fig. 12.

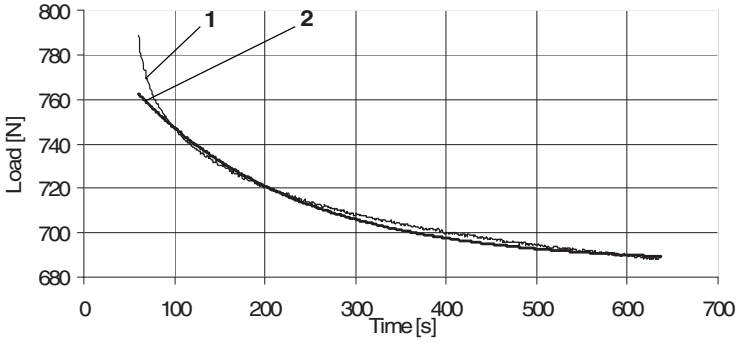

Fig. 12. Stress relaxation curves: the theoretical curve for the *Standard II* ideal material model and the experimental curve, both describing EPUR 90

The curves in Fig. 12 indicate that the *Standard II* model with the predetermined coefficients, i.e. $k_1 = 1.069 \cdot 10^5$ N/m, $k_2 = 6.865 \cdot 10^5$ N/m and $C_1 = 1.884 \cdot 10^7$ Ns/m, describes the analyzed material, EPUR 90, quite well (better than in the case of EPUR 95), although in the first seconds of the process there were some differences, like in the previous case. At the beginning of the process, the difference was about 3.2 % and gradually diminished to a few tenths of a percent.

4. Conclusion

This study was conducted first to analyze the effect of the coefficient of damping of the seal material on the parameters of its operation and then to describe the selected engineering material (polyurethane) by means of the *Standard II* material model. The results confirm the suitability of ideal material models for pictorial purposes, simulations and theoretical considerations as well as in engineering practice, for various calculations.

It can be concluded that a real material can be described with high accuracy in a specified range by means of an ideal material equation. In this study, the coefficients of the *Standard II* model equation were determined in such a way that the theoretical relaxation curves corresponded to the real (experimental) curves in the specified ranges of parameters. As shown in Section 2, the experimentally determined coefficients of the ideal material equation can be used to compare, with some predetermined accuracy, the general model with the real engineering material.

As illustrated in Section 1, the ideal material can also be used to perform an analysis for a seal model so that it is then possible to select the most suitable engineering material with parameters ensuring maximum damping of vibrations.

The above considerations were based on only one model, i.e. *Standard II*. It should be mentioned, however, that this method can be used for multi-parameter models of ideal materials.

Acknowledgement

The preparation of this paper was supported by the Ministry of Science and Higher Education through grant NN502 4498 33.

References

[1] Osiecki J.: *Fundamentals of the analysis of mechanical vibrations* (in Polish). Politechnika Świętokrzyska. Kielce 1979.

[2] Hernández-Jimenéz A., Hernández-Santiago J., Marcias-Garcia A., Sánchez-González J.: *Relaxation modulus in PMMA and PTFE fitting by fractional Maxwell model.* Polymer Testing, 2002, Volume 21, Issue 3, pp. 325-331.

[3] Chan Y.L., Ngan A.H.W.: *Invariant elastic modulus of viscoelastic materials measured by rate-jump tests.* Polymer Testing, 2010, Volume 21, Issue 5, pp. 558-564.

[4] Green, I., and Etsion, I.: *Nonlinear Dynamic Analysis of Noncontacting Coned-Face Mechanical Seals,* ASLE Transactions, 1986, Vol.29, pp. 383-393.

[5] Person V., Tournerie B., Frěne J.: *A Numerical Study of the Stable Dynamic Behavior of Radial Face Seals With Grooved Faces,* ASME Journal of Tribology, 1997, Vol. 119, pp. 507-514.

[6] Kundera Cz.: *Determination and Analysis of Cross-Couplings of Axial and Angular Vibrations of a Flexibly Mounted Ring in a Non-Contacting Face Seal.* ASME Journal of Tribology, 2003, Vol.125, No.4, pp.797-803.

[7] Bochnia J., Osiecki J.W.: *Model of dynamics of a face seals with consideration of the visco-elastic properties of the sliding ring.* 7th Conference on Dynamical Systems; Theory and Applications. Łódź, 2003, Proceedings vol.2, pp. 525-534.

[8] Bochnia J., Osiecki J.W.: *A model of the face seal dynamics with rheological properties of the sliding ring* (in Polish), Problemy Eksploatacji No 2, 2004, pp. 63-74.

[9] Bochnia J.: *A dynamic model of a face seal with a nonlinearly elastic sliding ring* (in Polish). Zeszyty Naukowe Politechniki Rzeszowskiej No 197, Mechanika z. 60 Problemy Dynamiki Konstrukcji, Rzeszów 2002, pp. 27-33.

[10] Osiecki J.: *Selected aspects of modeling in dynamic mechanical analysis* (in Polish). Dynamika Maszyn, Ossolineum PAN, Wrocław, 1974, pp. 12-48.